Hedging Volatility: Different Perspectives Compared

Richard Ogg

A dissertation submitted to the Faculty of Commerce, University of Cape Town, in partial fulfilment of the requirements for the degree of Master of Philosophy.

July 25, 2020

MPhil in Mathematical Finance,
University of Cape Town.

Declaration

I declare that this dissertation is my own, unaided work. It is being submitted for the Degree of Master of Philosophy in the University of the Cape Town. It has not been submitted before for any degree or examination in any other University.

July 25, 2020

Abstract

The accuracy of the Black and Scholes (1973) delta and vega neutral portfolio for a vanilla option was compared to a benchmark set by the Heston (1993) model in a stochastic volatility environment. The Black-Scholes portfolio was implemented using a fixed volatility and by implying volatility from the market. Additionally, a portfolio based on the Dupire (1994) local volatility model was also compared. It was found that a portfolio consisting of two short maturity options with matching maturities was best hedged by the Black-Scholes model when using implied volatility. This result was not maintained when the two options had mismatching maturities as the proportional differences in the vegas no longer cancelled. Further examination was completed on the type of financial instruments used to hedge volatility, comparing portfolios that consisted of an additional option and a variance swap to offset any vega. It was found that both hedged the option well, with similar accuracies.

Acknowledgements

I would like to thank my supervisor, Alex Backwell for the generosity of his time and expertise throughout the dissertation. Additionally, to AIFMFM, who have provided myself and others incredible opportunities both in and outside of the lecture halls. Finally, to all my peers in AIFMRM for keeping morale high and giving new perspectives when needed.

Contents

List of Figures

List of Tables

Chapter 1

Introduction

Volatility is one of the key parameters in option pricing and is often used to quote options instead of their monetary value. These implied volatilities create surfaces over a range of strikes and maturities with smiles and skews present, indicating that volatility is not constant in the way that the classical Black and Scholes (1973) model assumes. An alternative to the Black-Scholes model is the canonical Heston (1993) model. The model's popularity is due to its tractable form of incorporating both stochastic volatility and a stochastic stock process in option pricing.

With volatility being such a key variable in pricing options, it is common practice to hedge it. This dissertation answers the question: how accurately does the Black-Scholes hedge portfolio perform in a world where volatility is stochastic? The stochastic world will be simulated and priced using the Heston model. A hedged portfolio based on the Heston model sensitivities will act as a benchmark to which three alternative portfolios will be compared. The first is the Black-Scholes model, where, although the model assumes constant volatility, the sensitivity to the fixed volatility parameter is used in constructing the portfolio. The second portfolio makes use of implied volatility which is the volatility that calibrates the Black-Scholes model to the market. The last portfolio is based on the Dupire (1994) local volatility model, which provides a time varying volatility driven by instantaneous sensitivities to the option value.

A result of the stochastic nature of volatility in financial markets is the introduction of variance swaps. Before its introduction, hedging volatility was performed with an option that used volatility as a secondary parameter. Now, volatility can be hedged with an instrument where volatility provides the underlying value. Therefore, an analysis of the variance swap hedge compared to an option-based hedge will be completed.

To summarise the results, it was initially found that the hedge portfolios for the Black-Scholes model (using both fixed and implied volatility) and the Dupire local volatility model converged to the Heston model portfolio as volatility became

more constant. However, this trend was only present for a portfolio consisting of two short-term options with matching maturities. Over short maturities, the vegas of the Black-Scholes and Heston model behaved similarly, but differed in proportionality. This proportionality was cancelled out when calculating the additional option position resulting in equivalent portfolios. Thereafter, the portfolio was changed so that the additional option had a longer maturity to avoid the errors cancelling out. This resulted in all the portfolios performing poorly in hedging an option under stochastic volatility. With regards to hedging volatility with a variance swap, it was found that similar accuracies were achieved in comparison to the option-based volatility hedge.

An overview of this dissertation is as follows, Chapter 2 introduces option pricing in the context of non-constant volatility. In Chapter 3, vanilla options and variance swaps are priced and derived under stochastic volatility. These pricing techniques are then validated in Chapter 4 with the use of Monte Carlo simulations along with finite difference approximations to confirm the accuracy of the derived sensitivities. In Chapter 5, accuracies of the hedge portfolios making use of fixed, implied and local volatility models are compared in a stochastic volatility environment with the Heston model setting the benchmark. Additionally, option-based volatility hedging and variance swap-based hedging were compared. Finally, Chapter 6 concludes on the findings throughout this dissertation.

Chapter 2

Option Pricing

The financial industry has evolved throughout time and numerous option-based instruments have been developed to meet the needs of the market. In this dissertation, vanilla options on equities will be the main focus, with time-t prices given by the expectation under the risk-neutral measure and are of the following form:

$$V_t = \mathrm{E}_t^{\mathbb{Q}}[\alpha e^{-r(T-t)}(S_T - K)^+], \tag{2.1}$$

which is a function of the underlying stock price (S) at maturity (T) and strike (K). Along with the risk-free rate (r) which is assumed constant and α which indicates the type of option, either a put ($\alpha = -1$) or a call ($\alpha = 1$).

Looking at Equation 2.1, modelling the underlying is key to accurately price an option. The following stochastic differential equation (SDE) captures many of the popular techniques:

$$dS_t = rS_t dt + \sqrt{v_t} S_t dW_t^{(S)}, \tag{2.2}$$

with v_t representing the variance of the stock over a given period, r representing the drift in the risk-neutral world and $W_t^{(S)}$ being the Brownian motion that drives the random stock movement.

2.1 Modelling Volatility

In reality, volatility surfaces implied from market prices form smiles and skews as depicted in Figure 2.1. These trends arise for a variety of reasons, the main one being that in most models such as geometric Brownian motion (GBM) which assumes constant volatility in Equation 2.2 (i.e. $\sqrt{v_t} = \sigma_S$) it suggests that log-stock returns are normally distributed. However, it is a stylized-fact that distributions of log-stock returns are leptokurtic, as fatter tails and higher peaks are experienced in the markets. The fatter tails are a result of the Black-Scholes model underestimating extreme market movements (positive or negative). To account for these fatter tails, practitioners increase the volatility for far in or out of the money options. This

creates the curvature in the implied volatility surfaces known as the volatility smile as seen in the left panel of Figure 2.1. Skews on the other hand, arise from an in-balance in demand for options at either higher or lower strikes depending on market conditions. The most common reason for skews is that low cost put options are purchased by wealth managers to prevent severe losses in the event of a market crash. This excessive purchasing on the lower spectrum of strikes increases the value of the options which in turn results in higher volatilities being implied shown by the right panel of Figure 2.1.

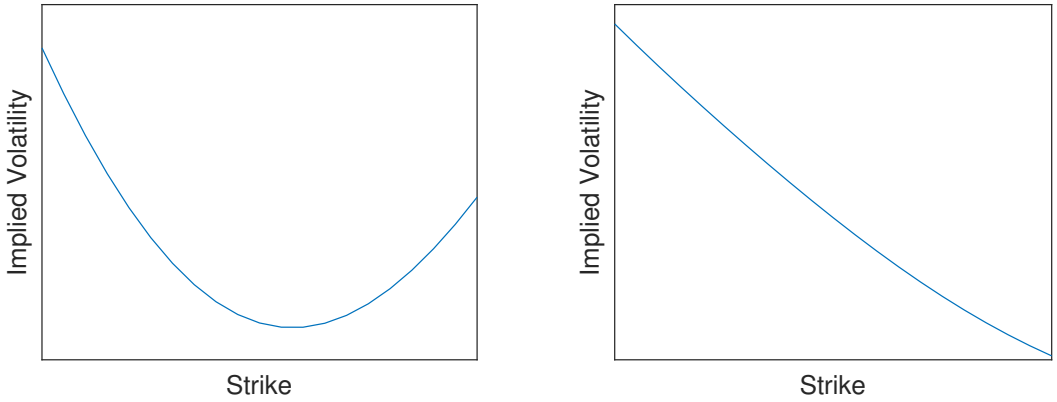

Fig. 2.1: Implied volatility smile and skew.

2.1.1 Deterministic Models

The simplest case of volatility is the Black-Scholes model which assumes that volatility of the stock is known and constant over the life of the option ($\sqrt{v_t} = \sigma_S$). The simplifying assumption of constant volatility, combined with GBM results in an easy to use and simple option pricer, with time-t prices given by

$$V_t^{\text{BS}} = \alpha[S_t\Phi(\alpha d_1) - Ke^{-r(T-t)}\Phi(\alpha d_2)], \tag{2.3}$$

where $\Phi(x)$ is the cumulative standard normal distribution evaluated at x with d_1 and d_2 defined as

$$d_1 = \frac{\ln\frac{S_t}{K} + (r + \frac{1}{2}\sigma_S^2)(T-t)}{\sigma_S\sqrt{T-t}} \quad \text{and} \quad d_2 = d_1 - \sigma_S\sqrt{T-t}.$$

Even though the model is simple and easy to use, simplifying volatility to a constant may be inadequate. To account for this, implied volatility (σ_{imp}) is an alternative approach. Implied volatility is the volatility that calibrates the Black-Scholes model to market prices and is a function of strike and maturity. Practitioners often

quote options in terms of implied volatility rather than quoting in price, because an option is traded to hedge risks or the trader has a view on future movements which is effectively taking a position on future volatility. Obtaining the implied volatility works as follows:

$$V^{\text{Market}}(K,T) = V^{\text{BS}}(K,T,\sigma_{\text{imp}}),$$

where σ_{imp} is the desired value to make the equation hold. An additional method is a local volatility (σ_{loc}) model which provides an instantaneous and time dependent volatility. The local volatility model derived by Dupire (1994) is one of the more widely used models and is given as

$$\sigma_{\text{loc}}(K,T) = \sqrt{\frac{\frac{\partial}{\partial T}V(K,T) + rK\frac{\partial}{\partial K}V(K,T)}{\frac{1}{2}K^2\frac{\partial^2}{\partial T^2}V(K,T)}}.$$

2.1.2 Stochastic Models

Similar to the stock process, variance can be modelled with an SDE of the following format (Wilmott, 2013):

$$dv_t = p(S,v_t,t)dt + q(S,v_t,t)dW_t^{(v)}, \tag{2.4}$$

which requires an additional Brownian motion term ($W_t^{(v)}$) that can be correlated to that of the stock dynamics ($W_t^{(S)}$). The functions $p(\cdot)$ and $q(\cdot)$ heavily influence the the dynamics of the volatility and are often calibrated so that the model can accurately price exchange traded options (Wilmott, 2013).

There are numerous stochastic variance models, but the main focus will be the dynamics outlined Cox *et al.* (1985) known as the CIR model, given by

$$dv_t = \kappa[\theta - v_t]dt + \sigma_v\sqrt{v_t}dW_t^{(v)}. \tag{2.5}$$

The dynamics allow for the variance to move randomly with σ_v representing the volatility of movements. Cox *et al.* (1985) also ensured that the variance is able to revert back to a mean level θ as seen in reality at rate κ.

2.2 The Greeks

The Greeks of an option are measures of the sensitivity of an option's value to its underlying determining parameters. In any option portfolio, controlling these sensitivities are crucial to understanding and managing portfolio risk. Although there are many Greeks, the sensitivity towards the underlying and the volatility will be the focus and are known as the option delta (Δ) and vega (ν) respectively.

The Black-Scholes (BS) Greeks are the sensitivities of the Black-Scholes option value outlined by Equation 2.3 and are given as

$$\Delta^{\text{BS}} = \frac{\partial V_t}{\partial S_t} = \alpha\Phi(\alpha d_1) \quad \text{and}$$

$$\nu^{\text{BS}} = \frac{\partial V_t}{\partial \sigma_S} = S_t\sqrt{T-t}\phi(d_1),$$

where $\phi(x)$ is the standard normal probability density function evaluated at x. Recall that $\alpha = 1$ indicates a call option and $\alpha = -1$ represents a put.

With the introduction of stochastic variance (v_t), further parameters are incorporated into pricing such as the volatility of variance (σ_v). To avoid any ambiguity and to maintain comparability to the Black-Scholes Greeks, the delta will still be the sensitivity toward the stock price (S_t) and the vega will be sensitivity toward the stochastic volatility ($\sqrt{v_t}$).

In the chapter to follow, it will be shown that the hedging of an option requires these delta and vega values to be neutralised to zero.

Chapter 3

Heston Model

Heston (1993) combines the risk-neutral dynamics of both the CIR model (Equation 3.2) along with stock price dynamics (Equation 3.1) to form the canonical Heston model:

$$dS_t = rS_t dt + \sqrt{v_t} S_t dW_t^{(S)} \quad \text{and} \tag{3.1}$$

$$dv_t = \kappa[\theta - v_t]dt + \sigma_v \sqrt{v_t} dW_t^{(v)}. \tag{3.2}$$

The Heston model's popularity is due to the fact that it combines both stochastic stock and volatility processes while maintaining tractability.

In Section 3.1, the focus will be on vanilla option pricing using the Heston model. The Heston model and its respective Greeks will be derived along with a description as to how they will be implemented. Thereafter, Section 3.2 moves onto pricing variance swaps which are more exotic instruments. The equations derived by Zhu and Lian (2011) are outlined and the sensitivities are determined.

3.1 Vanilla Options

3.1.1 Pricing

As with the Black-Scholes model, the Heston model pricer can be derived via two approaches - risk-neutral valuation and through portfolio replication. Both resulting in the same equation, but this dissertation will concentrate on the latter as it will provide intuition on option hedging. After the Heston partial differential equation (PDE) is obtained through a replication argument and estimating the form of the characteristic function, the PDE for the characteristic function can be determined. Solving this PDE produces a closed-form solution of the characteristic function. Thereafter, with the help of Fourier transforms, the Heston model option pricer will be determined.

To start the Heston PDE derivation, a portfolio (Π_t) is constructed to remove any uncertainty from an option $V_t^{(1)}$. To accomplish this, positions in two instru-

ments will be required as there are now two Brownian motions ($W_t^{(S)}$ & $W_t^{(v)}$) with correlation ρ. The two instruments will be an additional vanilla option represented by $V_t^{(2)}$ and the underlying stock (S_t) as depicted in the portfolio

$$\Pi_t = V_t^{(1)} + n_1 S_t + n_2 V_t^{(2)}. \tag{3.3}$$

The differential of the portfolio is given by

$$d\Pi_t = dV_t^{(1)} + n_1 dS_t + n_2 dV_t^{(2)},$$

with the dynamics of the option price obtained using Ito's lemma given as

$$dV_t = \frac{\partial V_t}{\partial t}dt + \frac{\partial V_t}{\partial S_t}dS_t + \frac{\partial V_t}{\partial v_t}dv_t + \frac{1}{2}\frac{\partial^2 V_t}{\partial S_t^2}(dS_t)^2 + \frac{1}{2}\frac{\partial^2 V_t}{\partial v_t^2}(dv_t)^2 + \frac{\partial^2 V_t}{\partial S_t \partial v_t}dS_t dv_t$$

and substituting the dynamics of the share and variance, and given that $dW_t dt = 0$, $(dt)^2 = 0$ and $dW_t^{(S)} dW_t^{(v)} = \rho dt$, the following results:

$$\begin{aligned} d\Pi_t = &\left[\frac{\partial V_t^{(1)}}{\partial t} + \frac{1}{2}v_t S_t^2 \frac{\partial^2 V_t^{(1)}}{\partial S_t^2} + \rho\sigma_v v_t S_t \frac{\partial^2 V_t^{(1)}}{\partial S_t \partial v_t} + \frac{1}{2}\sigma_v^2 v_t \frac{\partial^2 V_t^{(1)}}{\partial v_t^2}\right] dt \\ &+ n_2 \left[\frac{\partial V_t^{(2)}}{\partial t} + \frac{1}{2}v_t S_t^2 \frac{\partial^2 V_t^{(2)}}{\partial S_t^2} + \rho\sigma_v v_t S_t \frac{\partial^2 V_t^{(2)}}{\partial S_t \partial v_t} + \frac{1}{2}\sigma_v^2 v_t \frac{\partial^2 V_t^{(2)}}{\partial v_t^2}\right] dt \\ &+ \left[\frac{\partial V_t^{(1)}}{\partial S_t} + n_2 \frac{\partial V_t^{(2)}}{\partial S_t} + n_1\right] dS_t + \left[\frac{\partial V_t^{(1)}}{\partial v_t} + n_2 \frac{\partial V_t^{(2)}}{\partial v_t}\right] dv_t. \end{aligned} \tag{3.4}$$

To ensure no Brownian motion terms can affect the portfolio, positions in the additional option (n_2) and stock (n_1) will be calculated as follows:

$$\frac{\partial V_t^{(1)}}{\partial v_t} + n_2 \frac{\partial V_t^{(2)}}{\partial v_t} = 0 \implies n_2 = -\frac{\partial V_t^{(1)}}{\partial v_t} \Big/ \frac{\partial V_t^{(2)}}{\partial v_t} \quad \text{and}$$

$$\frac{\partial V_t^{(1)}}{\partial S_t} + n_2 \frac{\partial V_t^{(2)}}{\partial S_t} + n_1 = 0 \implies n_1 = -\left(n_2 \frac{\partial V_t^{(2)}}{\partial S_t} + \frac{\partial V_t^{(1)}}{\partial S_t}\right).$$

This results in the portfolio having no local sensitivity to the underlying and the variance.

Now that all the randomness has been removed from the portfolio, by a no-arbitrage argument it should be equivalent to the value of a portfolio increasing at the risk-free rate, r ($d\Pi_t = r\Pi_t dt$). Combining these positions along with Equation 3.4 and the fact that the portfolio is increasing at the risk-free rate, the following results:

$$\begin{aligned} r\Pi_t = &\left[\frac{\partial V_t^{(1)}}{\partial t} + \frac{1}{2}v_t S_t^2 \frac{\partial^2 V_t^{(1)}}{\partial S_t^2} + \rho\sigma_v v_t S_t \frac{\partial^2 V_t^{(1)}}{\partial S_t \partial v_t} + \frac{1}{2}\sigma_v^2 v_t \frac{\partial^2 V_t^{(1)}}{\partial v_t^2}\right] \\ &+ n_2 \left[\frac{\partial V_t^{(2)}}{\partial t} + \frac{1}{2}v_t S_t^2 \frac{\partial^2 V_t^{(2)}}{\partial S_t^2} + \rho\sigma_v v_t S_t \frac{\partial^2 V_t^{(2)}}{\partial S_t \partial v_t} + \frac{1}{2}\sigma_v^2 v_t \frac{\partial^2 V_t^{(2)}}{\partial v_t^2}\right]. \end{aligned} \tag{3.5}$$

This can be rearranged so that all terms involving the two instruments ($V_t^{(1)}$ & $V_t^{(2)}$) are on opposite sides of the equation as follows:

$$\text{LHS} = \frac{\frac{\partial V_t^{(1)}}{\partial t} + \frac{1}{2}v_t S_t^2 \frac{\partial^2 V_t^{(1)}}{\partial S_t^2} + \rho\sigma_v v_t S_t \frac{\partial^2 V_t^{(1)}}{\partial v_t \partial S_t} + \frac{1}{2}\sigma_v^2 v_t \frac{\partial^2 V_t^{(1)}}{\partial v_t^2} - rV_t^{(1)} + rS_t \frac{\partial V_t^{(1)}}{\partial S_t}}{\frac{\partial V_t^{(1)}}{\partial v_t}} \text{ and}$$

$$\text{RHS} = \frac{\frac{\partial V_t^{(2)}}{\partial t} + \frac{1}{2}v_t S_t^2 \frac{\partial^2 V_t^{(2)}}{\partial S_t^2} + \rho\sigma_v v_t S_t \frac{\partial^2 V_t^{(2)}}{\partial v_t \partial S_t} + \frac{1}{2}\sigma_v^2 v_t \frac{\partial^2 V_t^{(2)}}{\partial v_t^2} - rV_t^{(2)} + rS_t \frac{\partial V_t^{(2)}}{\partial S_t}}{\frac{\partial V_t^{(2)}}{\partial v_t}}.$$

The left hand side (LHS) of the equation is only a function of $V_t^{(1)}$ and similarly, the right hand side (RHS) of $V_t^{(2)}$. This implies that both the LHS and RHS can be written as a function $f(S_t, v_t, t)$. To obtain a PDE describing option value, Heston (1993) stipulates the structure as

$$f(S_t, v_t, t) = -\kappa^*(\theta^* - v_t) + \lambda(S_t, v_t, t), \tag{3.6}$$

where $\lambda(S_t, v_t, t)$ is the price of volatility risk along with κ^* and θ^* representing the real-world parameters. An application of Breeden (1979) consumption model gives a price of volatility risk that is a linear function of volatility, resulting in $\lambda(S_t, v_t, t) = \lambda v_t$, where λ is a constant. Furthermore, Heston (1993) also gives the parameters for the risk-neutral dynamics as

$$\kappa = \kappa^* + \lambda \quad \text{and} \quad \theta = \frac{\kappa^*\theta^*}{\kappa^* + \lambda}.$$

Combining the above with a generalised version of LHS or RHS, the following Heston PDE results:

$$\frac{\partial V_t}{\partial t} + \frac{1}{2}v_t S_t^2 \frac{\partial^2 V_t}{\partial S_t^2} + \rho\sigma_v v_t S_t \frac{\partial^2 V_t}{\partial v_t \partial S_t} + \frac{1}{2}\sigma_v^2 v_t \frac{\partial^2 V_t}{\partial v_t^2} - rV_t + rS_t \frac{\partial V_t}{\partial S_t} + \kappa(\theta - v_t)\frac{\partial V_t}{\partial v_t} = 0. \tag{3.7}$$

The boundary conditions for Equation 3.7 hold for a vanilla call option $V_t(S_t, v_t, t)$ with maturity T and strike K. At expiry, the option is valued based on its intrinsic value as follows:

$$V_T(S_T, v_T, T) = \max(0, S_T - K).$$

If the stock price is zero, the option has no value:

$$V_t(0, v_t, t) = 0.$$

As the stock price increases toward infinity, delta approaches one as given by

$$\frac{\partial}{\partial S_t} V_t(\infty, v_t, t) = 1$$

and when the volatility increases, the call option becomes equal to the stock price as follows:

$$V_t(S_t, \infty, t) = S_t.$$

Moving onto the characteristic function derivation, it is now convenient to give the option price as a function of $x_t = \ln S_t$ instead of the the asset value itself. Thus, a new PDE results:

$$\frac{\partial V_t}{\partial t} + \frac{1}{2} v_t \frac{\partial^2 V_t}{\partial x_t^2} + \rho\sigma_v v_t \frac{\partial^2 V_t}{\partial v_t \partial x_t} + \frac{1}{2}\sigma_v^2 v_t \frac{\partial^2 V_t}{\partial v_t^2} - rV_t + (r - \frac{1}{2}v_t)\frac{\partial V_t}{\partial x_t} + [\kappa(\theta - v_t)]\frac{\partial V_t}{\partial v_t} = 0. \tag{3.8}$$

By analogy to the Black-Scholes formula, Heston (1993) estimated a solution of a vanilla call option of the form:

$$V_t(T, K) = e^{x_t} P_1(x_t, v_t, t) - Ke^{-r(T-t)} P_2(x_t, v_t, t).$$

This was substituted into the required partial derivatives of Equation 3.8 to obtain a PDE of the probilities (P_1 and P_2) given by

$$\frac{\partial P_j}{\partial t} + \frac{1}{2} v_t \frac{\partial^2 P_j}{\partial x_t^2} + \rho\sigma_v v_t \frac{\partial^2 P_j}{\partial v_t \partial x_t} + \frac{1}{2}\sigma_v^2 v_t \frac{\partial^2 P_j}{\partial v_t^2} + (r + c_j v_t)\frac{\partial P_j}{\partial x_t} + (a - b_j v_t)\frac{\partial P_j}{\partial v_t} = 0,$$

where $c_1 = \frac{1}{2}$, $c_2 = -\frac{1}{2}$, $a = \kappa\theta$, $b_1 = \kappa + \lambda - \rho\sigma_v$ and $b_2 = \kappa + \lambda$.

Heston (1993) postulated that the characteristic function of the logarithm of the terminal share price could be described with a log linear function of the format

$$\phi_j(u, v_t, x_t, t) = e^{A_j(t,u) + B_j(t,u)v_t + iux_t}. \tag{3.9}$$

The characteristic function will adhere to the same PDE as that of its probabilities which is due to the Feyman-Kac theorem, resulting in a PDE of ϕ_j as

$$\frac{\partial \phi_j}{\partial t} + \frac{1}{2} v_t \frac{\partial^2 \phi_j}{\partial x_t^2} + \rho\sigma_v v_t \frac{\partial^2 \phi_j}{\partial v_t \partial x_t} + \frac{1}{2}\sigma_v^2 v_t \frac{\partial^2 \phi_j}{\partial v_t^2} + (r + c_j v_t)\frac{\partial \phi_j}{\partial x_t} + (a - b_j v_t)\frac{\partial \phi_j}{\partial v_t} = 0.$$

Substituting the differentials of the proposed characteristic function and rearranging gives

$$v_t\left(\frac{\partial B_j}{\partial t} + iu\rho\sigma_v B_j - \frac{1}{2}u^2 + \frac{1}{2}\sigma_v^2 B_j^2 + iuc_j - b_j B_j\right) + \frac{\partial A_j}{\partial t} + iur + aB_j = 0,$$

resulting in two differential equations. The first a Riccati equation of B_j, given by

$$\frac{\partial B_j}{\partial t} = -iu\rho\sigma_v B_j + \frac{1}{2}u^2 - \frac{1}{2}\sigma_v^2 B_j^2 - iuc_j + b_j B_j$$

and the second, a simple ODE for A_j

$$\frac{\partial A_j}{\partial t} = -iur - aB_j,$$

which is solved by integrating over time, bounded by the maturity (T) and current time (t). The solution of the Ricatti equation was given by Rouah (2013) as

$$B_j = \frac{b_j - iu\rho\sigma_v + d_j}{\sigma_v^2}\frac{1 - e^{d_j(T-t)}}{1 - g_j e^{d_j(T-t)}}, \tag{3.10}$$

where

$$d_j = \sqrt{(iu\rho\sigma_v - b_j)^2 - \sigma_v^2(2iuc_j - u^2)} \quad \text{and} \quad g_j = \frac{b_j - iu\rho\sigma_v + d_j}{b_j - iu\rho\sigma_v - d_j}.$$

Finally integrating the ODE results in

$$A_j = iur(T-t) + \frac{a}{\sigma_v^2}\left[(b_j - iu\rho\sigma_v + d_j)(T-t) - 2\ln\left(\frac{1 - g_j e^{d_j(T-t)}}{1 - g_j}\right)\right], \tag{3.11}$$

which provides the final function for the Heston characteristic function.

Combining Equation 3.10 and 3.11 with Equation 3.9, two characteristic functions result. The reason being that the complex root of d has two symmetrical values, one positive and one negative resulting in parameters differing by only an addition or subtraction operation. Albrecher *et al.* (2007) re-examined this and proved that although the Heston characteristic function works over a wide range of parameters there are cases that result in oscillations, slow dampening and even discontinuities resulting in poor numerical evaluation of the integral. Albrecher *et al.* (2007) adjusted the Heston characteristic functions into a single, more stable equation known as the Little Heston Trap characteristic function given by

$$\phi_{\ln(S_T)}(u) = e^{C(u) + D(u)v_0 + iu\ln(S_T)}, \tag{3.12}$$

where

$$C = iurT + \theta\kappa\left[Tx_- - \frac{1}{f}\ln\left(\frac{1 - me^{-Tl}}{1 - m}\right)\right] \quad \text{and}$$

$$D = \frac{1 - e^{-lT}}{1 - me^{-lT}}x_-,$$

with

$$f = \frac{\sigma_v^2}{2},$$

$$h = \kappa - iu\rho\sigma_v,$$

$$l = \sqrt{h^2 - 4fs},$$

$$m = \frac{x_-}{x_+},$$

$$x_{\pm} = \frac{h \pm l}{2f} \quad \text{and}$$

$$s = -\frac{u^2 + iu}{2}.$$

The characteristic function can now be inverted through a Fourier transform to determine the required probabilities for pricing an option. The option value will take the following form:

$$V_t = Ke^{-r(T-t)}(\beta - P_2) - S_t(\beta - P_1), \tag{3.13}$$

where $P_1 = \mathbb{Q}^S(S_T > K)$ and $P_2 = \mathbb{Q}(S_T > K)$ with β indicating the type of option, either a put ($\beta = 1$) or a call ($\beta = 0$). $\mathbb{Q}$ is the risk-neutral measure with the cash account (A_t) as the numéraire, whereas $\mathbb{Q}^S$ makes use of the stock price (S_t) as the numéraire.

The probabilities in Equation 3.13 can be calculated through a Fourier transform of the corresponding characteristic function. The formula derived by Gil-Pelaez (1951) accomplishes this, for any random variable x_T, with characteristic function ϕ_{x_T}, the probability of it exceeding a level k can be represented as

$$\Pr(x_T > k) = \frac{1}{2} + \frac{1}{\pi}\int_0^\infty \text{Real}\left[\frac{e^{-iuk}\phi_{x_T}(u)}{iu}\right] du. \tag{3.14}$$

P_2 can be computed simply with the Equation 3.14, using $x_T = \ln(S_T)$ and $k = \ln(K)$ as $\ln(\cdot)$ is a monotonic function as follows:

$$P_2 = \frac{1}{2} + \frac{1}{\pi}\int_0^\infty \text{Real}\left[\frac{e^{-iu\ln(K)}\phi_{\ln(S_T)}(u)}{iu}\right] du.$$

Before P_1 can be calculated the characteristic function of $\ln(S_T)$ under $\mathbb{Q}^S$ is required. The measure change from $\mathbb{Q}$ to $\mathbb{Q}^S$ is completed by

$$f^{\mathbb{Q}^S} ds = \frac{d\mathbb{Q}^S}{d\mathbb{Q}} f^{\mathbb{Q}} ds,$$

with

$$\frac{d\mathbb{Q}^S}{d\mathbb{Q}} = \frac{S_T/S_0}{A_T/A_0} = \frac{e^{\ln(S_T)}}{\phi_{\ln(S_T)}(-i)}.$$

This results in the characteristic function under the measure $\mathbb{Q}^S$, given by

$$\phi^S_{\ln(S_T)}(u) = \frac{\phi_{\ln(S_T)}(u-i)}{\phi_{\ln(S_T)}(-i)}.$$

Therefore,

$$P_1 = \frac{1}{2} + \frac{1}{\pi}\int_0^\infty \text{Real}\left[\frac{e^{-iu\ln(K)}\phi_{\ln(S_T)}(u-i)}{iu\phi_{\ln(S_T)}(-i)}\right] du.$$

3.1.2 The Greeks

As with the Black-Scholes model, the Heston model's Greeks can be determined through differentiation. The sensitivity with respect to the volatility is of the form:

$$\frac{dV_t}{d\sqrt{v_t}} = S_t \frac{dP_1}{d\sqrt{v_t}} - Ke^{-r(T-t)} \frac{dP_2}{d\sqrt{v_t}}.$$

With the sensitivity of P_2 to volatility being

$$\frac{dP_2}{d\sqrt{v_t}} = \frac{1}{\pi} \int_0^\infty \text{Real}[\frac{e^{-iu\ln(K)}}{iu} \frac{d\phi_{\ln(S_T)}(u)}{d\sqrt{v_t}}]du$$

and its respective characteristic function derivative given by

$$\frac{d\phi_{\ln(S_T)}(u)}{d\sqrt{v_t}} = 2\sqrt{v_t} D(u) \phi_{\ln(S_T)}(u).$$

Similarly, the sensitivity of P_1 to volatility is

$$\frac{dP_1}{d\sqrt{v_t}} = \frac{1}{\pi} \int_0^\infty \text{Real}[\frac{e^{-iu\ln(K)}}{iu} \frac{d}{d\sqrt{v_t}} \frac{\phi_{\ln(S_T)}(u-i)}{\phi_{\ln(S_T)}(-i)}]du$$

and applying the quotient rule to the characteristic function for P_1 results in

$$\frac{d}{d\sqrt{v_t}} \frac{\phi_{\ln(S_T)}(u-i)}{\phi_{\ln(S_T)}(-i)} = \frac{\phi_{\ln(S_T)}(-i) \frac{d\phi_{\ln(S_T)}(u-i)}{d\sqrt{v_t}} - \phi_{\ln(S_T)}(u-i) \frac{d\phi_{\ln(S_T)}(-i)}{d\sqrt{v_t}}}{\phi^2_{\ln(S_T)}(-i)}.$$

The sensitivity to the underlying can similarly be determined and takes the form:

$$\frac{dV_t}{dS_t} = P_1 + S \frac{dP_1}{dS_t} - \beta - Ke^{-rT} \frac{dP_2}{dS_t}.$$

With the sensitivity of P_2 to the underlying being

$$\frac{dP_2}{dS_t} = \frac{1}{\pi} \int_0^\infty \text{Real} \left[\frac{e^{-iu\ln(K)}}{iu} \frac{d\phi_{\ln(S_T)}(u)}{dS_t} \right] du,$$

with the differential of the characteristic function with respect to the underlying given by

$$\frac{d\phi_{\ln(S_T)}(u)}{dS_t} = \frac{iu}{S_t} \phi_{\ln(S_T)}(u)$$

and the sensitivity of P_1 to the underlying is

$$\frac{dP_1}{dS_t} = \frac{1}{\pi} \int_0^\infty \text{Real} \left[\frac{e^{-iu\ln(K)}}{iu} \frac{d}{dS_t} \frac{\phi_{\ln(S_T)}(u-i)}{\phi_{\ln(S_T)}(-i)} \right] du.$$

Once again, applying the quotient rule to the differential of the characteristic function for P_1, but with respect to the underlying results in the following:

$$\frac{d}{dS_t} \frac{\phi_{\ln(S_T)}(u-i)}{\phi_{\ln(S_T)}(-i)} = \frac{\phi_{\ln(S_T)}(-i) \frac{d\phi_{\ln(S_T)}(u-i)}{dS_t} - \phi_{\ln(S_T)}(u-i) \frac{d\phi_{\ln(S_T)}(-i)}{dS_t}}{\phi^2_{\ln(S_T)}(-i)}.$$

3.1.3 Implementation

Like the Black-Scholes equation, P_1 and P_2 can be evaluated numerically. One such method is that the integral can be evaluated using central quadrature as follows:

$$P_1 = \frac{1}{2} + \frac{1}{\pi}\sum_{n=1}^{N} \text{Real}\left[\frac{e^{-iu_n \ln(K)}\phi_{\ln(S_T)}(u_n - i)}{iu_n\phi_{\ln(S_T)}(-i)}\right]\delta_u \quad \text{and}$$

$$P_2 = \frac{1}{2} + \frac{1}{\pi}\sum_{n=1}^{N} \text{Real}\left[\frac{e^{-iu_n \ln(K)}\phi_{\ln(S_T)}(u_n)}{iu_n}\right]\delta_u,$$

where $u_n = (n - \frac{1}{2})\delta_u$ and δ_u representing the change in u. This same approach can be applied to numerically evaluate the Greeks in Section 3.1.2.

Rouah (2013) also suggests alternative forms of implementation, one being a discretisation scheme such as the Milstein scheme for the stock over time intervals of δ_t given as follows:

$$S_{t_i} = \begin{cases} S_0 & \text{if } i = 0, \\ S_{t_{i-1}} e^{(r - \frac{1}{2}v_{t_{i-1}})\delta_t + \sqrt{v_{t_{i-1}}\delta_t} z_{S,i}} & \text{if } i > 0, \end{cases}$$

with the variance discretisation given by

$$v_{t_i} = \begin{cases} v_0 & \text{if } i = 0, \\ (v_{t_{i-1}} + \kappa(\theta - v_{t_{i-1}})\delta_t + \sigma_v\sqrt{v_{t_{i-1}}\delta_t} z_{v,i} + \frac{1}{4}\sigma_v^2(z_{v,i}^2 - 1)\delta_t)^+ & \text{if } i > 0, \end{cases}$$

where $z_{v,i}$ and $z_{S,i}$ are random numbers drawn from the standard normal distribution with correlation ρ. The reflection is not part of the Milstein scheme, but the variance process is able to produce values below zero. Lord *et al.* (2010) names multiple methods to prevent negative variances, with the absolute value being the safest.

The discretisation will enable stock and variance paths to be determined. This is important when validating the Heston model through a Monte Carlo simulation and when dynamically hedging an option.

3.1.4 Model Parameters

With volatility being stochastic, the Heston model can induce volatility smiles and skews which are experienced in reality. Figure 3.1 shows how the parameters in the dynamics of the CIR model affect the curvature of the volatility smiles and the extent of skew. Correlation of the two Brownian motions (ρ) is the main factor influencing the skew, with negative correlations resulting in negative skews and vice versa. The correlation is typically negative, reflecting the leverage effect (Bae

et al., 2007). Additionally, the rate of mean reversion (κ) and process volatility (σ_v) affect the depth of the smile. The σ_v is directly proportional to the size of the smile whereas κ has an inverse relationship. Furthermore, the level of mean reversion (θ) does not induce any excess skew or curvature, but rather determines the level of volatility.

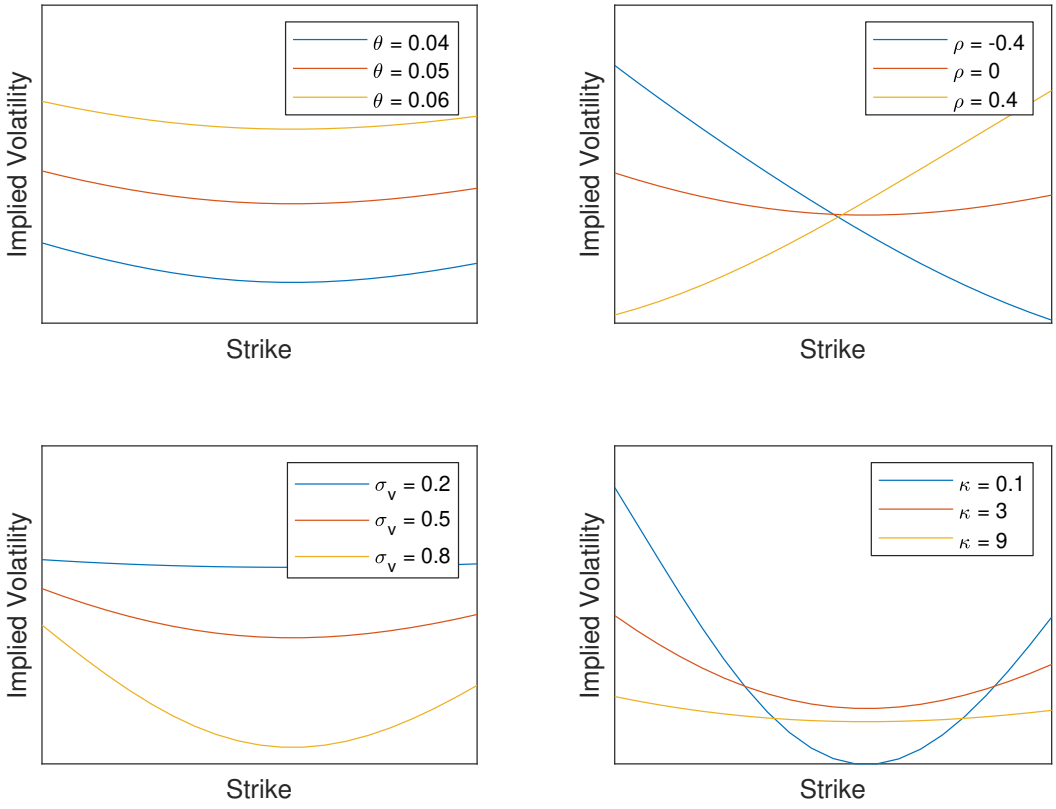

Fig. 3.1: Volatility smiles and skews in the Heston Model.

3.2 Variance Swaps

Another set of instruments used to trade volatility are variance swaps. These are forward contracts on a future realised variance (σ_R^2), with a payoff of

$$V_T = \omega(\sigma_R^2 - K_0^{\text{Var}})L,$$

with K_0^{Var} being the strike which is fixed at inception, nominal L and ω indicating the position, either long ($\omega = 1$) or short ($\omega = -1$) the swap. The realised variance

is the random component in variance swaps and is calculated based on the closing price of the stock at specific points in time as follows:

$$\sigma_R^2 = \frac{1}{T}\sum_{i=1}^{N}\left(\frac{S_{t_i} - S_{t_{i-1}}}{S_{t_{i-1}}}\right)^2 \times 100^2.$$

The number of measurements (N) and time interval (δ_t) between each measured value can differ and will be stipulated in the contract. This dissertation will assume equally spaced intervals of one trading day.

3.2.1 Pricing

Throughout the life of a swap, the time-t price can be given by the discounted risk-neutral expectation as follows:

$$V_t = \omega e^{-r(T-t)} E_t^{\mathbb{Q}}[\sigma_R^2 - K_0^{\text{Var}}]L.$$

Furthermore, forward contracts have equal downside and upside risk. Therefore, K_0^{Var} is set to ensure there is zero initial value ($V_0 = 0$) resulting in $K_0^{\text{Var}} = \mathrm{E}_0^{\mathbb{Q}}[\sigma_R^2]$. The value after inception (V_t) is calculated based on what the new variance strike K_t^{Var} should be to maintain the swap value at zero, given by

$$V_t = \omega e^{-r(T-t)}(K_t^{\text{Var}} - K_0^{\text{Var}})L.$$

Zhu and Lian (2011) derived an explicit closed-form solution which will be given without derivation:

$$K_t^{\text{Var}} = \mathrm{E}_t^{\mathbb{Q}}[\sigma_R^2] = \frac{e^{r\delta_t}}{T-t}\left[f(v_t) + \sum_{i=2}^{N_t} f_i(v_t)\right] \times 100^2.$$

The function $f(v_t)$ is used for the initial time interval and is given by

$$f(v_t) = e^{\widetilde{C}(\delta_t) + \widetilde{D}(\delta_t)v_t} + e^{-r\delta_t} - 2$$

and then $f_i(v_t)$ thereafter, which takes the form

$$f_i(v_t) = e^{\widetilde{C}(\delta_t) + \frac{\widetilde{c}_i e^{-\kappa t_{i-1}}}{\widetilde{c}_i - \widetilde{D}(\delta_t)}\widetilde{D}(\delta_t)v_t}\left(\frac{\widetilde{c}_i}{\widetilde{c}_i - \widetilde{D}(\delta_t)}\right)^{\frac{2\kappa\theta}{\sigma_v^2}} + e^{-r\delta_t} - 2.$$

The separation is due to the fact that at t_0 the initial values are known, but afterwards the expected values for the following time intervals need to be estimated. The additional functions are given by

$$\widetilde{C}(\delta_t) = r\delta_t + \frac{\kappa\theta}{\sigma_v^2}\left[(\widetilde{a} + \widetilde{b})\delta_t - 2\ln\left(\frac{1 - \widetilde{g}e^{\widetilde{b}\delta_t}}{1 - \widetilde{g}}\right)\right],$$

$$\widetilde{D}(\delta_t) = \frac{\widetilde{a}+\widetilde{b}}{\sigma_v^2}\left(\frac{1-e^{\widetilde{b}\delta_t}}{1-\widetilde{g}e^{\widetilde{b}\delta_t}}\right) \quad \text{and}$$

$$c_i = \frac{2\kappa}{\sigma_v^2(1-e^{-\kappa t_{i-1}})}.$$

Combined with the parameters calculated by

$$\widetilde{a} = \kappa - 2\rho\sigma_v,$$

$$\widetilde{b} = \sqrt{\widetilde{a}^2 - 2\sigma_v^2} \quad \text{and}$$

$$\widetilde{g} = \frac{\widetilde{a}^2}{\sigma_v^2} + \frac{\widetilde{a}}{\sigma_v}\sqrt{\frac{\widetilde{a}^2}{\sigma_v^2} - 2} - 1.$$

3.2.2 The Greeks

Like options, the sensitivity to parameters and variables can be computed for variance swaps. This dissertation concentrates on hedging the sensitivities to the stock price (delta) and volatility (vega). Looking at the formula derived by Zhu and Lian (2011), determining the expected realised variance requires no input of stock price, hence, variance swaps have no delta. On the other hand, the variance swap most definitely has a sensitivity towards the initial volatility as it is the underlying variable in the financial instrument. The derivative with respect to the volatility was computed as

$$\frac{\partial V_t}{\partial\sqrt{v_t}} = \omega e^{-r(T-t)}\frac{e^{r\delta_t}}{T-t}\left[\frac{\partial}{\partial\sqrt{v_t}}f(v_t) + \sum_{i=2}^{N_t}\frac{\partial}{\sqrt{v_t}}f_i(v_t)\right] \times 100^2 L,$$

with

$$\frac{\partial}{\partial\sqrt{v_t}}f(v_t) = 2\sqrt{v_t}\widetilde{D}(\delta_t)e^{\widetilde{C}(\delta_t)+\widetilde{D}(\delta_t)v_t} \quad \text{and}$$

$$\frac{\partial}{\partial\sqrt{v_t}}f_i(v_t) = 2\sqrt{v_t}\frac{\widetilde{c}_i e^{-\kappa t_{i-1}}}{\widetilde{c}_i - \widetilde{D}(\delta_t)}\widetilde{D}(\delta_t)e^{\widetilde{C}(\delta_t)+\frac{\widetilde{c}_i e^{-\kappa t_{i-1}}}{\widetilde{c}_i-\widetilde{D}(\delta_t)}\widetilde{D}(\delta_t)v_t}\left(\frac{\widetilde{c}_i}{\widetilde{c}_i-\widetilde{D}(\delta_t)}\right)^{\frac{2\kappa\theta}{\sigma_v^2}}.$$

Chapter 4

Model Validation

Before the hedge portfolios can be compared, the validity of the models are confirmed in this chapter. Since the Greeks are derivatives of a financial instrument's value with respect to a specific parameter, a finite difference approximation given by

$$\frac{df}{dx} \approx \frac{f(x+h) - f(x)}{h}, \tag{4.1}$$

will act as a point of comparison for the Greeks derived in Chapter 3. A small value for h will suffice as an approximation for the sensitivities.

The pricing models can be validated with Monte Carlo simulations which allow for the evaluation of an expectation, such as an option price or the realised variance, through random number sampling and computation. The more random numbers sampled, the more accurate the evaluation becomes. In both the Black-Scholes and Heston model, Brownian motion drives the randomness and thus sampling will be based on the standard normal distribution. As an example, the Monte Carlo for an option price looks as follows

$$V_t(T,K) = \alpha e^{-r(T-t)} \mathrm{E}_t^{\mathbb{Q}}[(S_T - K)^+] \approx \alpha e^{-r(T-t)} \frac{1}{n} \sum_{i=1}^{n} \left[S_T(\bar{z}_i^{(S)}, \bar{z}_i^{(v)}) - K \right]^+,$$

where $\bar{z}_i^{(S)}$ and $\bar{z}_i^{(v)}$ are vectors of random numbers sampled from the standard normal distribution. Multiple random numbers are required for each sample path as the Milstein scheme outlined in Section 3.1.3 discretises time, resulting in multiple random numbers required to progress the stock and the variance process to maturity.

4.1 Option Pricer

The Heston characteristic function pricing method is compared with the Monte Carlo valuation obtained using the Milstein discretisation scheme as seen in Figure

4.1. The error bands are 3 standard deviations which decrease by the order $\frac{1}{\sqrt{n}}$ with n being the number of sample paths. It can be clearly seen that the Monte Carlo tends toward the estimation using the characteristic function method which confirms the function is operating appropriately.

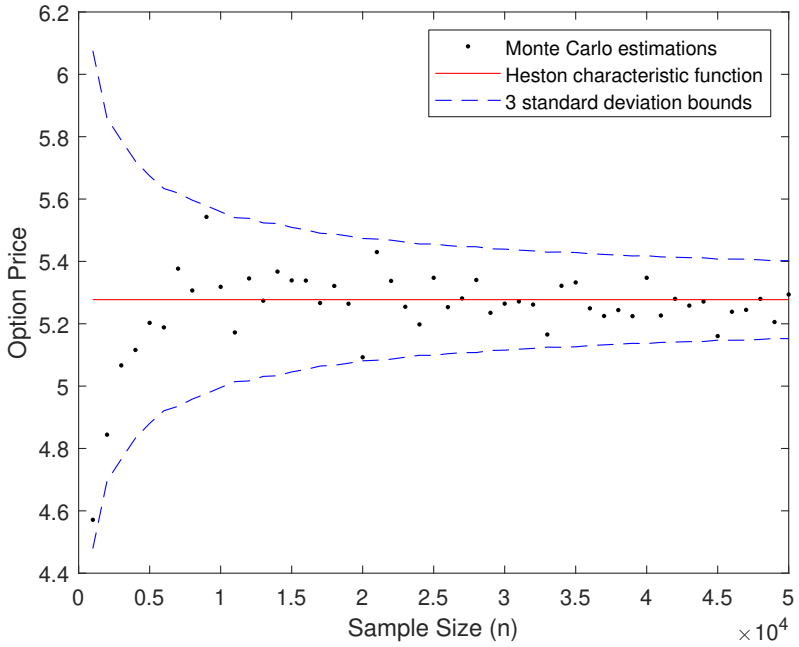

Fig. 4.1: Heston option pricer Monte Carlo ($S_0 = 100$, $K = 105$, $\rho = -0.4$, $v_0 = 0.06$, $\theta = 0.05$, $\kappa = 3$, $\sigma_v = 0.5$, $T = 0.5$ and $r = 3\%$).

The Greeks can be validated far more simply using Equation 4.1. As seen in Table 4.1, the finite difference approximations for both the delta and vega of the Heston model match what was derived, meaning the equations in Section 3.1.2 are behaving correctly.

Tab. 4.1: Validation of the Heston model's vega and delta ($S_0 = 100$, $K = 105$, $\rho = -0.4$, $v_0 = 0.06$, $\theta = 0.05$, $\kappa = 3$, $\sigma_v = 0.5$, $T = 0.5$ and $r = 3\%$).

Greek	Heston	Finite difference
Δ	0.482	0.482
ν	14.571	14.571

4.2 Variance Swap Pricer

The same validation was completed on the variance swap pricer given in Section 3.2. Once again, the Monte Carlo shown in Figure 4.2 proves that the realised variance is being calculated correctly and the Monte Carlo converges towards the closed-form solution derived by Zhu and Lian (2011).

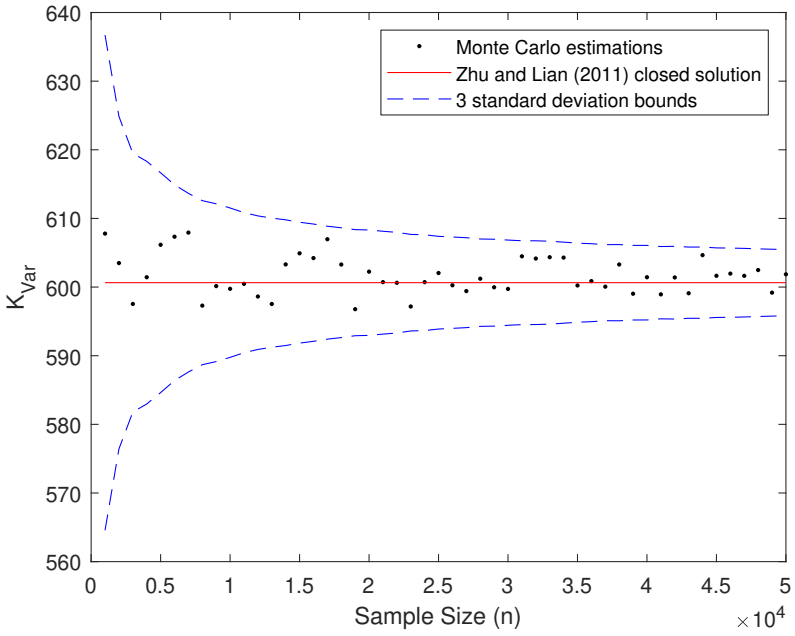

Fig. 4.2: Realised variance Monte Carlo ($v_0 = 0.06$, $\rho = -0.4$, $\theta = 0.06$, $\kappa = 3$, $\sigma_v = 0.5$, $T = 0.5$ and $r = 3\%$).

Similar to Section 4.1, the finite difference approximation and the sensitivity with respect to volatility derived in Section 3.2.2 matched as summarised in Table 4.2.

Tab. 4.2: Validation of the variance swap vega ($v_0 = 0.06$, $\rho = -0.4$, $\theta = 0.06$, $\kappa = 3$, $\sigma_v = 0.5$, $T = 0.5$ and $r = 3\%$).

Greek	Zhu and Lian (2011) closed-form	Finite difference
ν	2538	2538

Chapter 5

Volatility Hedging

The option being hedged ($V_t^{(1)}$) is a one month call option struck at 105 and will require two additional instruments ($I_t^{(1)}$ & $I_t^{(2)}$) to remove sensitivity with respect to the underlying and volatility. A hedge portfolio of the following format results:

$$\Pi_t = V_t^{(1)} + n_1 I_t^{(1)}(S_t, v_t) + n_2 I_t^{(2)}(S_t, v_t).$$

The vega will be neutralised in two manners - with an additional option ($I_t^{(2)} = V_t^{(2)}$) and a variance swap ($I_t^{(2)} = V_t^{\text{swap}}$) and the remaining delta is removed with the underlying stock ($I_t^{(1)} = S_t$). To achieve vega and delta neutral portfolios, the following equations need to be solved simultaneously to determine the required positions in the two hedge instruments (n_1 & n_2):

$$\Delta_{\text{T}} = \Delta_1 + n_1 \Delta_{I_1} + n_2 \Delta_{I_2} \quad \text{and}$$

$$\nu_{\text{T}} = \nu_1 + n_1 \nu_{I_1} + n_2 \nu_{I_2}.$$

Δ_T and ν_T are the target delta and vega of the portfolio which would be set to zero. Whereas, the deltas and vegas underscored by 1, I_1 and I_2 indicate the respective delta and vega for the option being hedged and instrument 1 and 2. In the case of the stock, its delta and vega will simply be 1 and 0 respectively. Therefore, the positions

$$n_1 = -(\Delta_1 + n_2 \Delta_{I_2}) \quad \text{and} \quad n_2 = -\frac{\nu_1}{\nu_{I_2}}$$

will be required to achieve a delta and vega neutral portfolio. Looking at the position in the stock, it can be seen that it is simply the reverse position of the sum of the deltas of the two options. The position in $I_t^{(2)}$ is simply a ratio of the vegas from the option being hedged and $I_t^{(2)}$.

In the comparison to follow, the Heston model and its respective hedge portfolio will act as a benchmark and will be used to evaluate the accuracy of the three alternative portfolios. The portfolios being compared are the Black-Scholes model that uses a fixed volatility, the Black-Scholes portfolio that implies volatility from

the market and the Dupire (1994) local volatility model. In both the Heston and Black-Scholes model, replicating the option requires continuous hedging. In reality, this is not achievable for two reasons; trading continuously is not possible and even if it were, the transaction costs to maintain such a portfolio will make the replication irrelevant. Therefore, practitioners try find a balance between cost effective trading and letting sensitivities depart from zero. The frequency of adjusting the hedge positions can range from once at inception known as static hedging to dynamically hedging up to twice a day depending on the size of the portfolio.

5.1 Option-based Hedging

When using an option to hedge volatility, the portfolio will be of the same format as in the Heston Model PDE derivation which ensured no sensitivity to the stock or the variance given by

$$\Pi_t = V_t^{(1)} + n_S S_t + n_2 V_t^{(2)}, \tag{5.1}$$

with the positions in the stock (n_S) and additional option (n_2) being

$$n_S = -(\Delta_1 + n_2 \Delta_2) \quad \text{and} \quad n_2 = -\frac{\nu_1}{\nu_2}.$$

The additional option will always be struck at the money and will initially have a maturity that matches the maturity of the option being hedged. Thereafter, the additional option will be continually purchased at a one year maturity and also struck at the money to see the effects of mismatching the maturities.

5.1.1 Static

The difference between the Black-Scholes and Heston model is that the Heston model does not assume variance as a constant variable, but rather a stochastic one that follows the CIR process (Equation 3.2). The properties of v_t are described by Rouah (2013) and it is shown that the process $2c_t v_t$ follows a non-central chi-squared distribution with $\frac{4\kappa\theta}{\sigma_v^2}$ degrees of freedom and a non-central parameter of $2c_t v_s e^{-\kappa(t-s)}$ with $c_t = \frac{2\kappa}{\sigma_v^2(1-e^{-\kappa(t-s)})}$, resulting in the expected value and variance of the variance process as follows:

$$\mathrm{E}[v_t \mid v_s] = \theta + (v_s - \theta)e^{-\kappa(t-s)} \quad \text{and} \tag{5.2}$$

$$\mathrm{V}[v_t \mid v_s] = \frac{v_s \sigma_v^2 e^{-\kappa(t-s)}}{\kappa}(1 - e^{-\kappa(t-s)}) + \frac{\theta\sigma_v^2}{2\kappa}(1 - e^{-\kappa(t-s)})^2. \tag{5.3}$$

Examining Equations 5.2 and 5.3, it can be seen that setting σ_v, the volatility of variance to zero, the random component of the variance falls away. This

turns the variance process into a deterministic process, but time varying model as $\mathrm{Var}[v_t \mid v_0] = 0$. Furthermore, setting θ to v_0, the variance process becomes time independent with $\mathrm{E}[v_t \mid v_0] = v_0$. Therefore, with θ equal to v_0 and σ_v set to 0, the Heston model collapses to the Black-Scholes model, with both having equivalent prices and hedge positions which is illustrated in Figure 5.1.

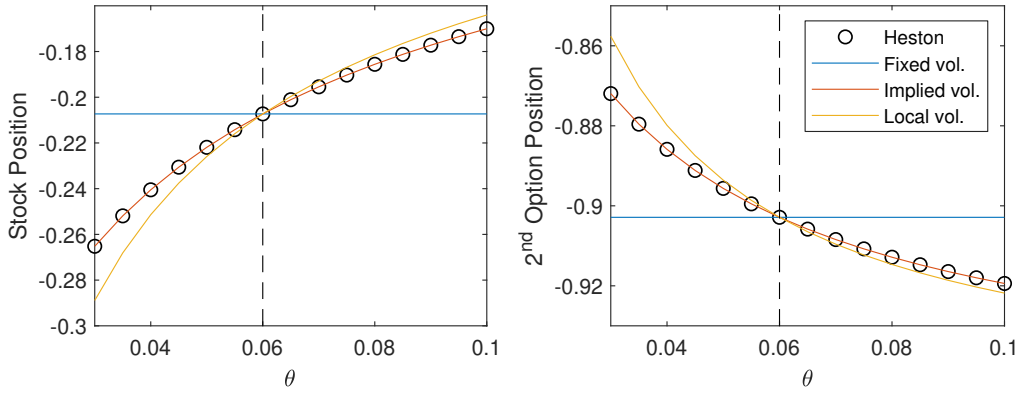

Fig. 5.1: Static hedge positions whilst varying θ ($S_0 = 100$, $K = 105$, $\rho = -0.4$, $\sigma_v = 0$, $v_0 = 0.06$, $\kappa = 3$, $T = 1$ and $r = 3\%$).

A similar argument can be made about κ, because it is the rate of mean reversion which is effectively how strong the pull back to the mean is. Thus, as it tends to infinity the variance of the variance process tends to zero, resulting in a constant process with an expected value tending toward θ. This trend can be visualised in Figure 5.2 below and even with a κ of 20, the hedge positions determined by the Heston model are well matched by all three alternative portfolios.

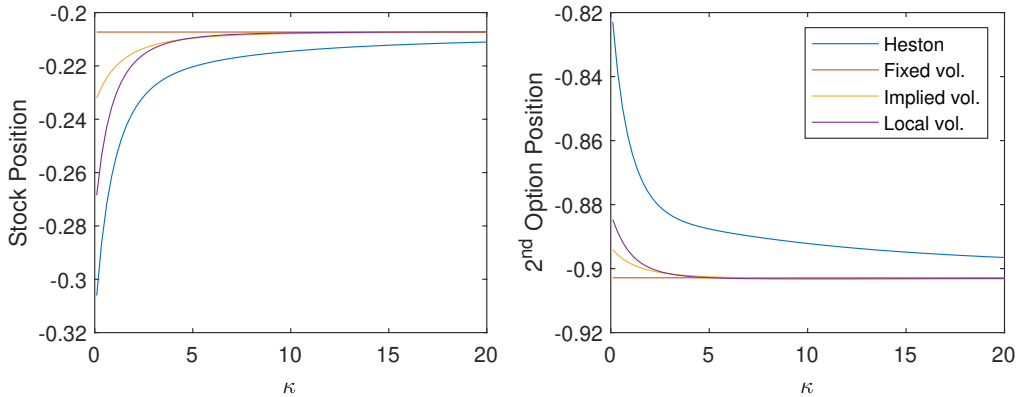

Fig. 5.2: Static hedge positions whilst varying κ ($S_0 = 100$, $K = 105$, $\rho = -0.4$, $v_0 = 0.06$, $\theta = 0.06$, $\sigma_v = 0.5$, $T = 1$ and $r = 3\%$).

Therefore, the effects of $\kappa \longrightarrow \infty$ is equivalent to the combination of $\theta = v_0$ and $\sigma_v = 0$. They are the main parameters that control the variability and expected value of the variance process. This is further emphasized with Figure 5.3 as it shows that the correlation (ρ) of the two Brownian motions become less significant as κ tends to infinity and thus, tending towards the Black-Scholes hedge positions. On the other hand, at lower values of κ, the randomness introduced has a greater effect since the drift is no longer dominating the dynamics in Equation 2.5. It can be seen that at positive correlations the Black-Scholes underestimates the hedge positions in the stock and over estimates with positive correlations. The reverse is true for the position in the additional option.

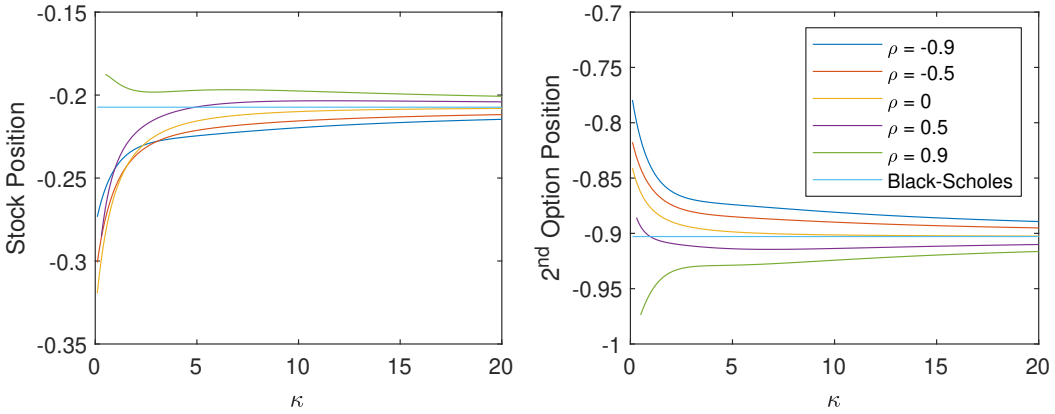

Fig. 5.3: Static hedge positions whilst varying κ and ρ ($S_0 = 100$, $K = 105$, $v_0 = 0.06$, $\theta = 0.06$, $\sigma_v = 0.5$, $T = 0.5$ and $r = 3\%$).

5.1.2 Dynamic

In the static case, fixed positions were taken in the hedging instruments over the life of the option being hedged. Whereas hedging dynamically requires re-balancing of the positions throughout the period of the option. The benefit of dynamic hedging is that positions are fixed for shorter time intervals so that they can be adapted based on current market conditions resulting in a more accurate hedge. Over each time interval, a change in portfolio value can occur due to the re-balancing as the value of the portfolio's instruments at the end of the interval could differ from the beginning. These value changes are accumulated and termed the profit and loss (P&L) of the hedge. Each change in value over the period t_{i-1} and t_i is calculated by subtracting the portfolio value at the beginning of the period ($\Pi_{t_{i-1}}$) from the value at the end of the period discounted to the beginning of the period $\left(\Pi_{t_i} e^{-r(t_i - t_{i-1})}\right)$. These changes are all discounted back to the current time (t_0) and summed to form

the overall P&L as follows:

$$\text{P\&L} = \sum_{i=1}^{N} \left(\Pi_{t_i} e^{-r(t_i - t_{i-1})} - \Pi_{t_{i-1}} \right) e^{-rt_{i-1}},$$

where $t_N = T$.

The P&L can be calculated for multiple sample paths and form a distribution which can be used to visually measures the accuracy of a hedge. To analyse more quantitatively, the sum of squares (SS) of the distributions will be compared. A characteristic of an accurate hedge is that the mean is centred around zero as no clear profits or losses are obtained as the portfolio consists of the option being hedged along with its replicating portfolio. Furthermore, the accuracy of the hedge can be quantified with the SS of the distribution which shows how concentrated it is over zero. The more concentrated over zero, the less profit or loss being incurred over the hedging period resulting in a higher hedge accuracy.

As mentioned previously, to achieve a perfect hedge, continuous trading is required. The P&L of a perfect hedge would be a point mass over zero, because no profit or loss is incurred. As frequency of re-positioning decreases, the P&L will begin to flatten and look normally distributed around zero. To demonstrate this effect and to prove to the reader that the P&L is behaving accordingly, the P&L for the Heston model was plotted at various frequencies as seen in Figure 5.4.

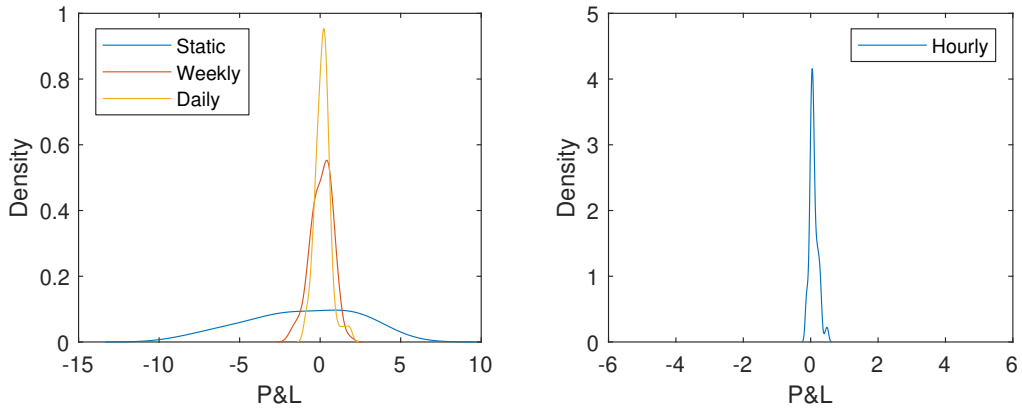

Fig. 5.4: Effect of re-balance frequency on P&L distribution ($S_0 = 100$, $K = 105$, $\rho = -0.4$, $v_0 = 0.06$, $\theta = 0.06$, $\kappa = 3$, $\sigma_v = 0.5$, $T = \frac{1}{12}$ and $r = 3\%$).

The P&L distributions provide a visual way to compare the accuracy of various hedging technique, from now on, the accuracy will be measured by the distributions sum of squares (SS). With a low SS indicating higher accuracy as long as the

mean is centred around zero. This is illustrated by Figure 5.5 which shows the sum of squares of Figure 5.4.

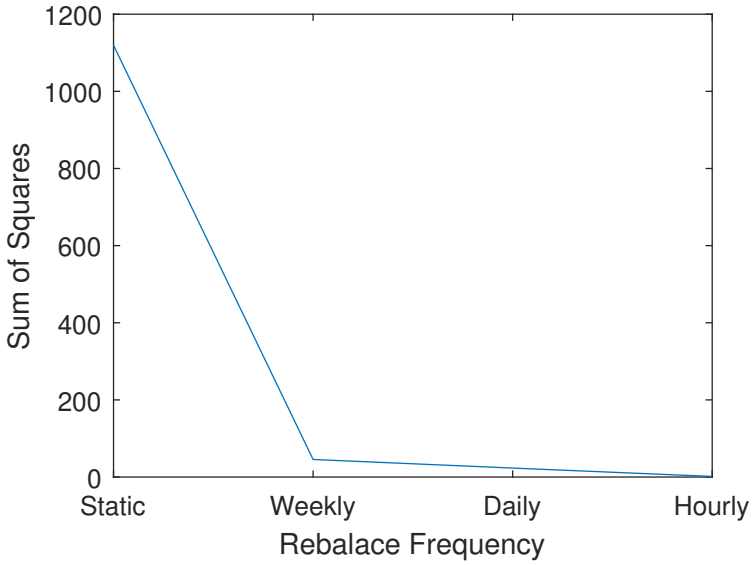

Fig. 5.5: Effect of re-balance frequency on sum of squares ($S_0 = 100$, $K = 105$, $\rho = -0.4$, $v_0 = 0.06$, $\theta = 0.06$, $\kappa = 3$, $\sigma_v = 0.5$, $T = \frac{1}{12}$ and $r = 3\%$).

Even though the frequency of re-balancing is an important factor, to achieve comparable and realistic results the hedge positions will be adjusted daily throughout the remainder of this dissertation.

The hedging techniques will be compared in various regimes that can be experienced by the market outline by Crépey (2004). Since, the Heston model parameters are usually calibrated to represent the markets volatility movements, the parameters can be varied to induce certain characteristics that the market experiences. The 3 regimes that will be of most significance are summarised in Table 5.1.

Tab. 5.1: Market regimes.

Regime 1	Constant (high κ and low σ_v) vs. volatile variance (low κ and high σ_v)
Regime 2	Decreasing ($\frac{\theta}{v_0} < 1$) vs. increasing variance ($\frac{\theta}{v_0} > 1$)
Regime 3	High (high θ and v_0) vs. low variance (low θ and v_0)

Matching Maturities

In this section, the option used to hedge the volatility ($V_t^{(2)}$) has the same maturity as the option being hedged ($V_t^{(1)}$). This portfolio will be referred to as 'matching maturities'.

The first market characteristic examined was how constant the variance process is, which can be controlled by the rate of mean reversion (κ). To recap the effect of κ, as it tends toward infinity, the pull towards θ becomes so significant that the variance process becomes constant. The κ effects combined with a high volatility ($\sigma_v = 0.9$) are illustrated on the left panel of Figure 5.6 and a low volatility ($\sigma_v = 0.1$) on the right panel. Starting with the high volatility, the implied volatility technique best matches the Heston model followed by the local volatility model and then the fixed volatility model. Although there is a significant difference at lower κ, as the κ increases, the rate of mean reversion begins to outweigh the volatility introduced and all models converge, because the volatility is becoming more constant. On the other hand, with a low volatility (right panel) it can be seen that even low κ are able to induce the effect of constant volatility resulting in all four models having highly similar sum of squares.

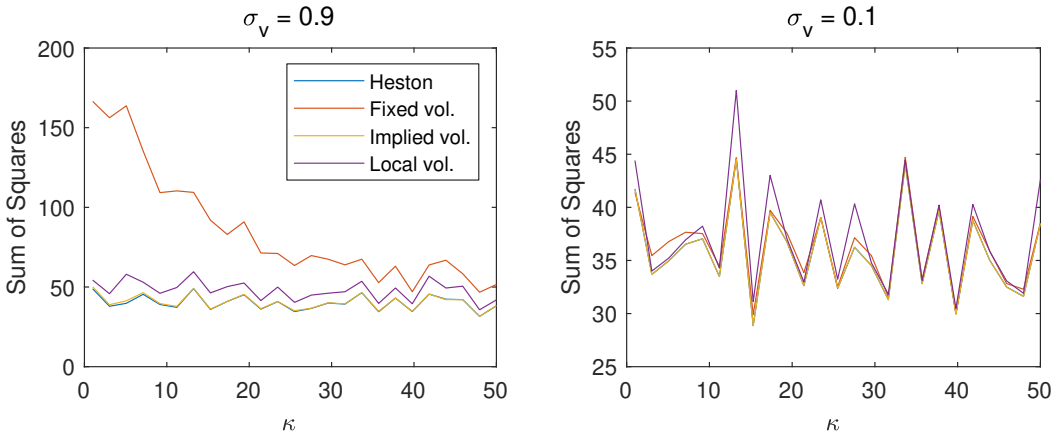

Fig. 5.6: Regime 1 effect on the sum of squares of the P&Ls ($S_0 = 100$, $K = 105$, $\rho = -0.4$, $v_0 = 0.06$, $\theta = 0.06$, $T = \frac{1}{12}$ and $r = 3\%$).

For the comparison in Regime 2, θ was varied from being a quarter of the initial variance to 5 times greater. Since θ is the level of mean reversion, when $\theta < v_0$ (or $\theta > v_0$) the variance process will decrease (or increase) towards θ at rate κ. The effect on the sum of squares of the P&L for an increasing/decreasing variance at a high volatility ($\sigma_v = 0.9$) is shown on the left panel of Figure 5.7 and the right panel illustrates the affect of low volatility ($\sigma_v = 0.1$). With increasing variance, the

accuracy of the fixed volatility portfolio diverges away from the benchmark set by the Heston model. Whereas, the implied volatility method matched the benchmark the best, closely followed by the local volatility model, throughout the range of θ. The right panel once again iterates the point made in the static section, with $\theta = v_0$ and σ_v being low, the variance process becomes constant. Therefore, when $\frac{\theta}{v_0} = 1$ the distribution's sum of squares converge.

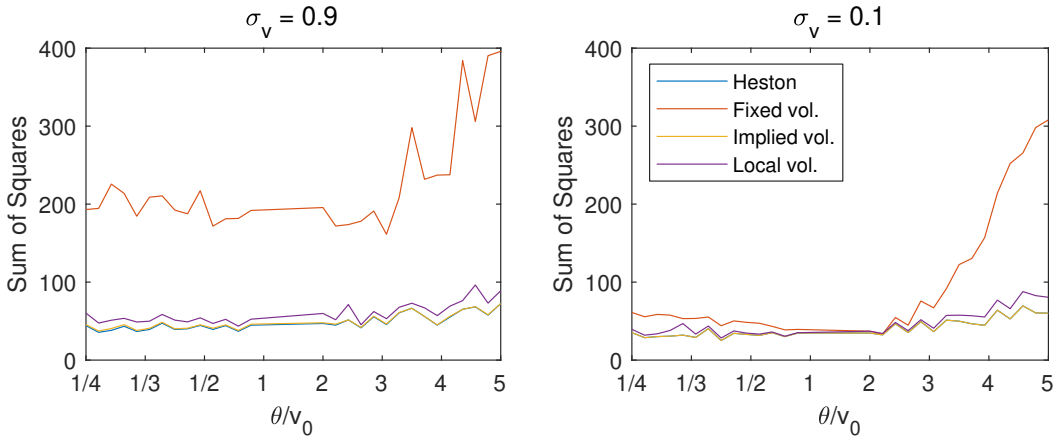

Fig. 5.7: Regime 2 effect on the sum of squares of the P&Ls ($S_0 = 100$, $K = 105$, $\rho = -0.4$, $v_0 = 0.06$, $\kappa = 3$, $T = \frac{1}{12}$ and $r = 3\%$).

With regards to Regime 3, it was found that higher levels of variance had little effect on the trends outlined in Figure 5.6 and 5.7. The trends were maintained, but the higher variances produced more variable P&Ls which is expected as the stock paths can increase and decrease significantly more than with a lower variance resulting in larger hedging error. This aligns with what was seen in Figure 5.7, at higher levels of θ it can be seen the sum of squares begins to increase as the mean variance level increases.

From the above discussion we can conclude that the most significant characteristic that differentiates the hedges is the volatility of the variance process. This can be controlled with κ and σ_v. Therefore, the hedge positions were analysed at a close to constant volatility ($\kappa = 50$ and $\sigma_v = 0.1$) and a volatile variance process ($\kappa = 1$ and $\sigma_v = 0.9$). The hedge positions varying through time depicted in Figure 5.8 are align with the results obtained from the sum of squares of the P&Ls. At constant volatility, the positions of all the models overlay each other resulting in similar accuracies of the hedge. Whereas the volatile variance process experiences substantially different hedge positions with the portfolio using fixed volatility clearly performing the worst.

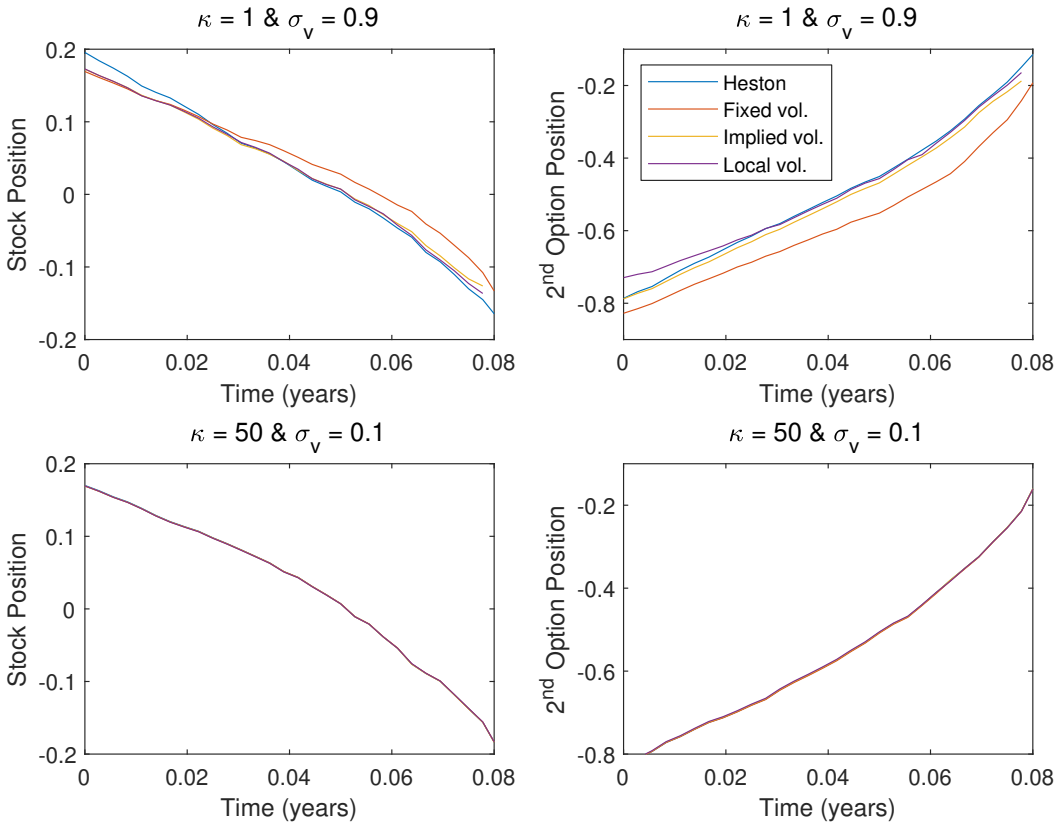

Fig. 5.8: Dynamic hedge positions with matched maturities ($S_0 = 100$, $K = 105$, $\rho = -0.4$, $v_0 = 0.06$, $\theta = 0.06$, $T = \frac{1}{12}$ and $r = 3\%$).

It may seem odd that the stock position to hedge the call option is out of the range of $[0, -1]$. However, there are two sources of delta - one from the option being hedged ($V_t^{(1)}$) and another from the additional option ($V_t^{(2)}$) to hedge the vega. The additional option can introduce or remove additional delta depending on the ratio of the two vegas.

The Greeks

The hedge positions are dependant on the Greeks as they are calculated solely based on the stock and volatility sensitivities. The additional option position will be analysed first as it is independent of the position in the stock and is controlled strictly by the vegas.

The trend over the range of strikes is consistent for both the Heston and Black-Scholes model as seen by Figure 5.9. Vega peaks at the money and moving further in or out of the money, the option becomes symmetrically less sensitive to volatility.

Looking at effects of κ, the vegas seem to decrease proportionally over the range of strikes as κ increases at short maturities even with respect to the Black-Scholes vega. This is understandable because a higher κ results in a stronger pull back to θ, so any change in the initial value will have less effect as the variance will return to the mean level faster. Since the position in the option is calculated based on the ratio of the vegas, the majority of the proportionality cancels resulting in similar option positions at a variety of parameter inputs for both the Heston and Black-Scholes portfolios. To illustrate this point, the two black squares indicate the Black-Scholes vegas for two options; a strike of 105 and a strike of 110. Similarly, the two red dots indicate the Heston vegas for the same two options described above. Visually, they seem to be in similar proportions which shows why the option positions are fairly consistent even though the vegas themselves can differ so drastically.

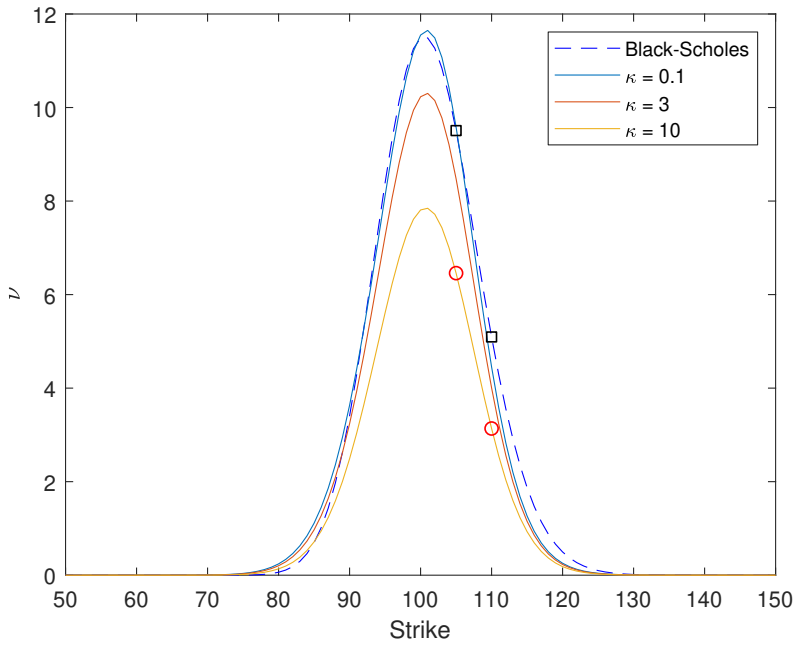

Fig. 5.9: Effect of moneyness and κ on ν ($S_0 = 100$, $\rho = -0.4$, $v_0 = 0.06$, $\theta = 0.06$, $\sigma_v = 0.5$, $T = \frac{1}{12}$ and $r = 3\%$).

Since the position in the additional option relies on a ratio of the two vegas, issues could arise when the proportionality no longer cancels. Figure 5.10 shows how the above trend is only maintained for short maturities, the vegas do not maintain their proportionality as maturity increases. This is due to a change in the initial volatility having different effects on the Heston and Black-Scholes vegas. The Black-Scholes vega will continually increase with an increase in the initial volatility

as the effects are permanent. On the other hand, the vegas from the Heston model increase fast, peak and then deteriorate to zero with κ effecting the rate of this deterioration. If the initial volatility increases, but θ remains the same, the volatility will revert to θ. With longer time horizons and higher rates of mean reversion, the variance has the opportunity to return to θ resulting in no effect to the option value in the long run. The proportionality or in this case lack thereof is no longer present and is illustrated with the two black squares (Black-Scholes) and the two red dots (Heston). They still both represent two options, but in this case they have different maturities and are all struck at the money. This could introduce problems when the option used to hedge the volatility is of a different maturity time.

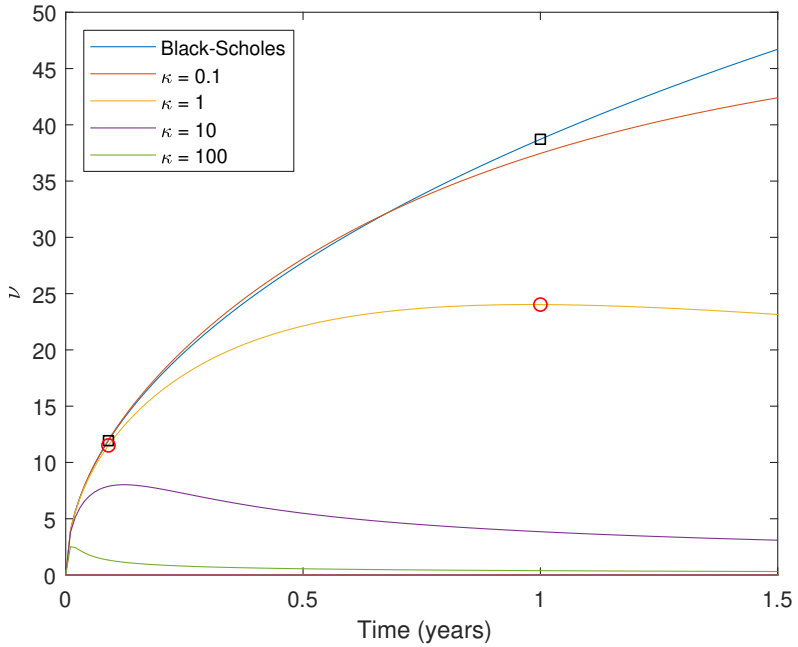

Fig. 5.10: Effect of time and κ on ν ($S_0 = 100$, $K = 105$, $\rho = -0.4$, $v_0 = 0.06$, $\theta = 0.06$, $\sigma_v = 0.5$ and $r = 3\%$).

Moving onto the stock position, which ensures delta neutrality. The deltas of the Black-Scholes and Heston model experience the same trend over a range of maturities, illustrated by Figure 5.11. As they both represent the probability that the stock will be greater than the strike (Bakshi *et al.*, 1997). When the option is highly likely to end in the money, the delta is close to one. The likelihood increases as the strike and maturity time decrease until the option expires. At expiry all that will remain is a step function showing the option was either in ($\Delta = 1$) or out the money ($\Delta = 0$).

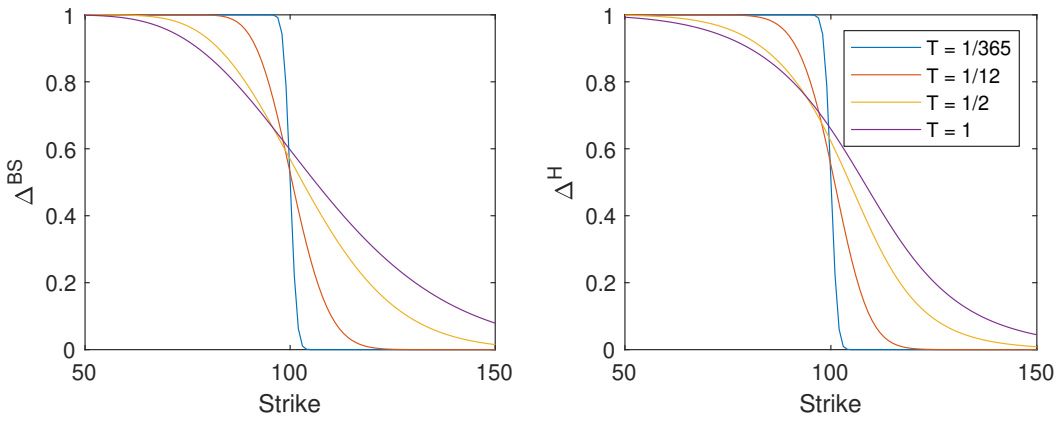

Fig. 5.11: Effect of moneyness and time on Δ ($S_0 = 100$, $\rho = -0.4$, $v_0 = 0.06$, $\theta = 0.06$, $\kappa = 3$, $\sigma_v = 0.5$ and $r = 3\%$).

Although the deltas experience the same trends, they do differ. The differences are referred to as hedge ratio bias by Kurpiel and Roncalli (1998) and they are highly dependent on the Heston model parameters and the maturity time. Once, again κ was varied and the difference between the Heston and Black-Scholes delta was taken over a range of strikes as seen by Figure 5.12. The same behaviour in the difference is experienced over the strike, with the κ accentuating this trend. As mentioned previously, the delta is effectively the probability that the option will be in the money, $\mathbb{Q}^S(S_t > K)$. So as the volatility becomes constant ($\kappa \to \infty$), the likelihood of ending in the money will be the same as the stock follows the dynamics of GBM, because volatility is now constant and thus, $\Delta^H \to \Delta^{BS}$. Furthermore, like the vegas previously, the Black-Scholes delta poorly represents the Heston model delta at longer maturity times and lower κ.

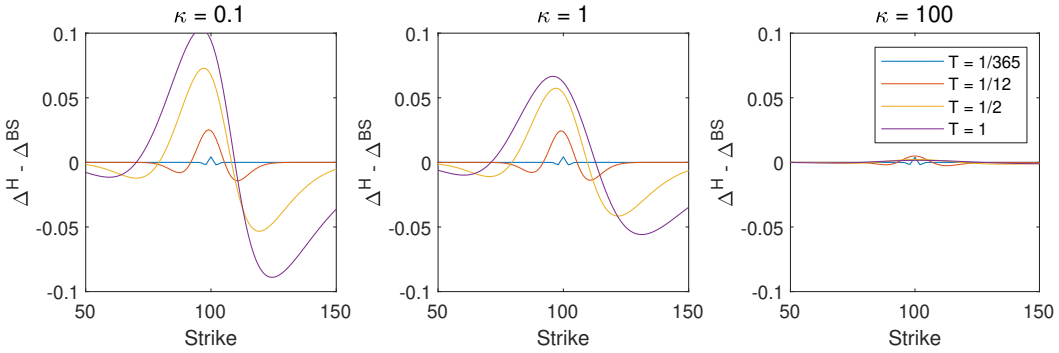

Fig. 5.12: Difference of the Heston and Black-Scholes Δ whilst varying moneyness at certain κ ($S_0 = 100$, $\rho = -0.4$, $v_0 = 0.06$, $\theta = 0.06$, $\sigma_v = 0.5$ and $r = 3\%$).

Maturity Mismatch

In this section, the option being hedged remains unchanged as a one month call option ($V_t^{(1)}$), whereas the option used to hedge the volatility ($V_t^{(2)}$) will now have a standard maturity of one year and will still be struck at the money. This portfolio will be referred to as a 'maturity mismatch'.

The reason for this adjustment is to compare the hedge portfolios when the proportionality of vegas is no longer present. Furthermore, although the 'matching maturity' portfolio is theoretically sound, in reality, the option used to hedge will depend on market liquidity. The most liquid options would act best as hedging instruments which would be at the money options with set maturities. Figure 5.13 demonstrates the accuracy of portfolios with mismatching maturities.

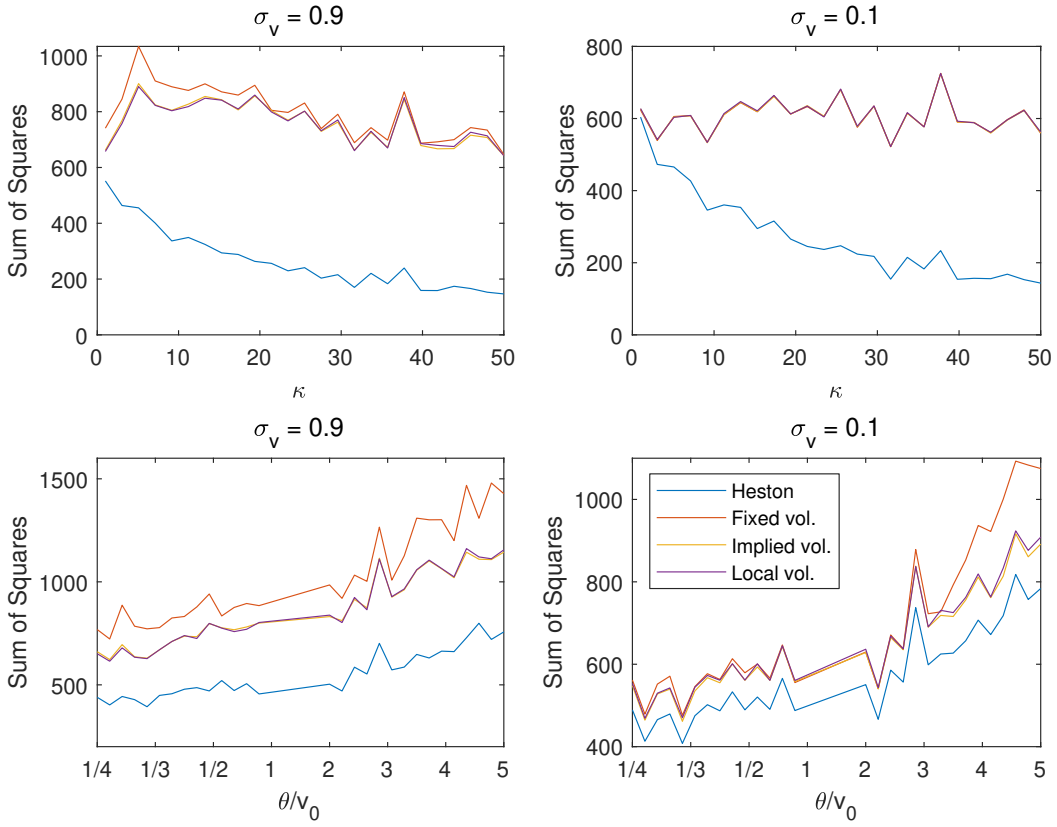

Fig. 5.13: Regime effect on the sum of squares of the P&Ls using mismatched maturities ($S_0 = 100$, $K = 105$, $\rho = -0.4$, $v_0 = 0.06$, $\theta = 0.06$, $\kappa = 3$, $T = \frac{1}{12}$ and $r = 3\%$).

All the alternative portfolios poorly match the accuracy of the Heston model in both Regimes. Furthermore, the only trend present from Figure 5.6 and 5.7 is that at high variance levels, the sum of squares increases because the hedging is discrete and the more volatile movements in prices result in greater profit and losses. To further emphasize the inadequacy of the Black-Scholes Greeks in comparison to Heston's with different maturities, Figure 5.14 was produced. In both scenarios (volatile variance and constant variance), all three methods of modelling volatility are substantially worse than the Heston model at determining the hedge positions and only converge closer to maturity. The convergence happens because the option being hedged will have very little vega resulting in a small position in the additional option. Similarly, the delta's will be fairly consistent as they will either most likely be in the money ($\Delta = 1$) or out the money ($\Delta = 0$).

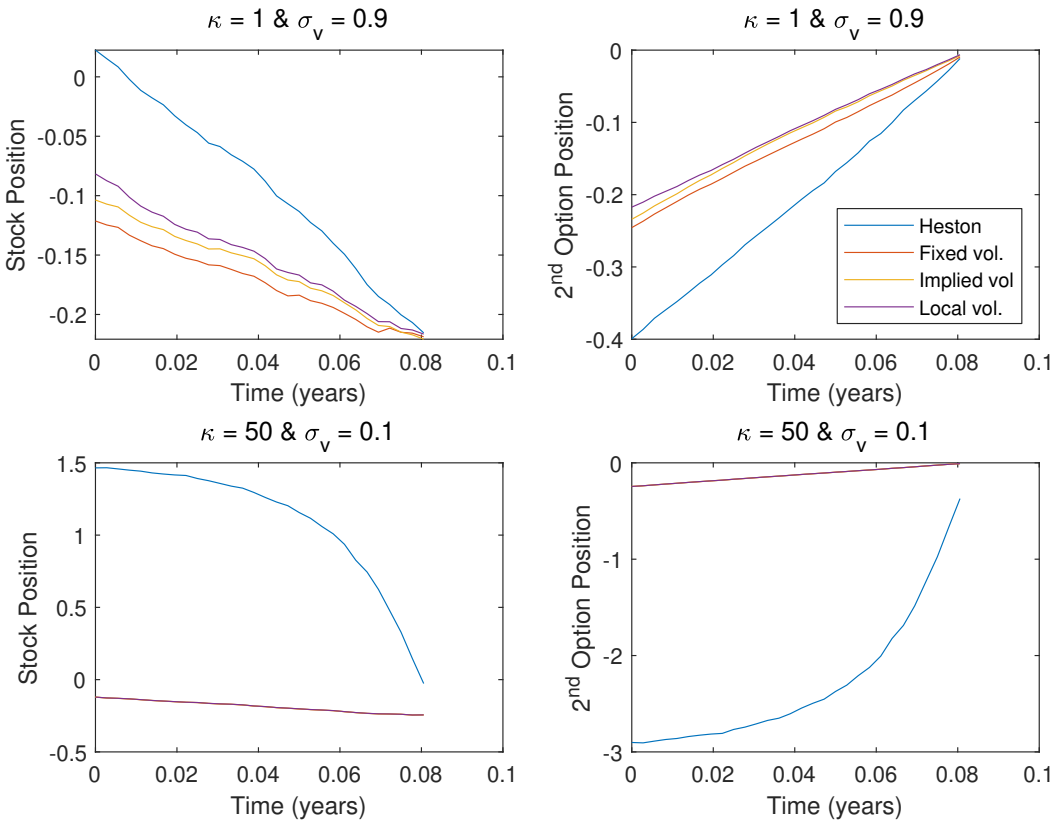

Fig. 5.14: Dynamic hedge positions with mismatched maturities ($S_0 = 100$, $K = 105$, $\rho = -0.4$, $v_0 = 0.06$, $\theta = 0.06$, $T = \frac{1}{12}$ and $r = 3\%$).

5.2 Variance Swap-based Hedging

The portfolio of an option being hedged with a variance swap is of a similar format to what was previously used, given by

$$\Pi_t = V_t^{(1)} + n_S S_t + n_{\text{swap}} V_t^{\text{swap}}.$$

The position in the variance swap (n_{swap}) is similarly calculated based on a ratio of the option and variance swap vegas as follows:

$$n_{\text{swap}} = -\frac{\nu_1}{\nu_{\text{swap}}}.$$

However, the position in the stock (n_S) to maintain delta neutrality will differ. Before, the instrument used to hedge volatility was an additional option which brought in further delta to be hedged. Variance swaps have no delta, even though realised variance is calculated based on a set of stock price measurements, they are only used to determine a weighted average of the variance and act as points of reference. Therefore, the position in the stock is simply the reverse of any delta from the option being hedged, given by

$$n_S = -\Delta_1.$$

It was shown that the Black-Scholes equation for vega is inaccurate at representing the Heston model's vega, especially with long maturity options. Therefore, this section will make use of the sensitivities from the Heston model to determine the positions in the hedge instruments.

The results of hedging volatility with another option in comparison to a variance swap are similar in accuracy as seen by the left panel of Figure 5.15 which shows the profit and loss distributions. The variance swap hedge is slightly more accurate with a sum of squares of 155 in comparison to the option-based hedge of 181. This difference is small and could reverse depending on the Heston parameters. The right panel of Figure 5.15 shows the capital required to maintain vega neutrality in each case. The variance swap-based volatility hedge is far less capital intensive in comparison to the option-based hedging. This is due to the fact that the underlying of a variance swap is the variance itself and has a far higher sensitivity to volatility than an option, where volatility is a secondary parameter. Furthermore, the realised variance is multiplied by 100^2 so the sensitivity is amplified. Since the variance swap has a far higher vega, the nominal value required in the variance swap is far lower than that of the option to achieve vega neutrality.

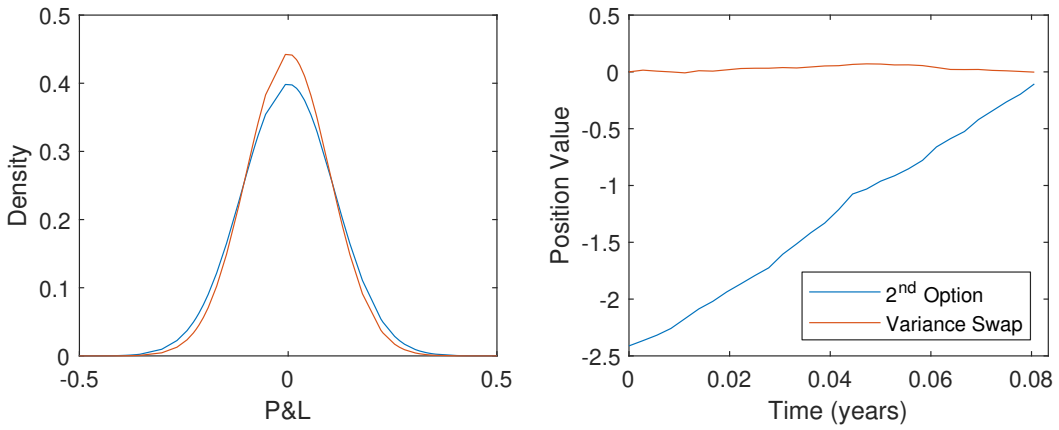

Fig. 5.15: Variance swap vs. option-based volatility hedging ($v_0 = 0.06$, $\theta = 0.06$, $\kappa = 3$, $\sigma_v = 0.5$, $\delta_t = \frac{1}{365}$, $T = \frac{1}{12}$ and $r = 3\%$).

Chapter 6

Conclusion

In a portfolio consisting of an option, an additional option position with matching maturities and a stock position, it was found that the Black-Scholes portfolio with volatility implied by the prevailing option prices, gave a portfolio that best matched the Heston model portfolio. Furthermore, when the stochastic volatility became more constant, all the models began to converge to the same portfolio regardless of the volatility model implemented.

It is interesting to note that although the Heston and the Black-Scholes deltas were highly similar over a range of strikes and maturities, the vegas experienced completely different trends. At shorter maturities, the Heston model vega behaved like the Black-Scholes vega, peaking at the money and deteriorating symmetrically as moneyness increased and decreased. The difference became apparent over longer maturity options as a change in volatility had different effects between the two models. The Black-Scholes model assumes constant volatility and the initial change will be present throughout the option's life, thus increasing the vega as maturity increases. The Heston model has a level of mean reversion (θ) that the variance will revert to. The longer the maturity or higher the κ, the faster the vega will reduce as the effect of an increase in volatility is minimised. Since the two options in the portfolio had the same maturity, these inaccuracies in the vega were removed due to their proportionality.

The portfolio was adapted so that the additional option maintained a maturity of one year to ensure no overlapping of maturities. In this format, all three alternative portfolios poorly matched the Heston model's benchmark. Finally, a variance swap was used to hedge the volatility of the option which was once again compared to the initial benchmark set. It was found that the variance swap portfolio performed slightly better as the variance swap has such a large sensitivity to volatility, requiring only a small investment to vega hedge and thus reducing the size of both profits and losses, resulting in a distribution more concentrated over zero.

Bibliography

Albrecher, H., Mayer, P., Schoutens, W. and Tistaert, J. (2007). The little Heston trap, *Wilmott* pp. 83–92.

Bae, J., Kim, C.-J. and Nelson, C. R. (2007). Why are stock returns and volatility negatively correlated?, *Journal of Empirical Finance* **14**(1): 41–58.

Bakshi, G., Cao, C. and Chen, Z. (1997). Empirical performance of alternative option pricing models, *The Journal of Finance* **52**(5): 2003–2049.

Black, F. and Scholes, M. (1973). The pricing of options and corporate liabilities, *Journal of Political Economy* **81**(3): 637–654.

Breeden, D. T. (1979). An intertemporal asset pricing model with stochastic consumption and investment opportunities, *The Journal of Financial Economics* **7**(2): 65–96.

Cox, J. C., Ingersoll Jr, J. E. and Ross, S. A. (1985). A theory of the term structure of interest rates, *Econometrica* **53**(2): 385–408.

Crépey, S. (2004). Delta-hedging vega risk?, *Quantitative Finance* **4**(5): 559–579.

Dupire, B. (1994). Pricing with a smile, *Risk* **7**(1): 18–20.

Gil-Pelaez, J. (1951). Note on the inversion theorem, *Biometrika* **38**(3-4): 481–482.

Heston, S. L. (1993). A closed-form solution for options with stochastic volatility with applications to bond and currency options, *The Review of Financial Studies* **6**(2): 327–343.

Kurpiel, A. and Roncalli, T. (1998). Option hedging with stochastic volatility, *Available at SSRN 1031927* .

Lord, R., Koekkoek, R. and Dijk, D. V. (2010). A comparison of biased simulation schemes for stochastic volatility models, *Quantitative Finance* **10**(2): 177–194.

Rouah, F. D. (2013). *The Heston Model and Its Extensions in Matlab and C#*, John Wiley & Sons.

Wilmott, P. (2013). *Paul Wilmott on Quantitative Finance*, John Wiley & Sons.

Zhu, S.-P. and Lian, G.-H. (2011). A closed-form exact solution for pricing variance swaps with stochastic volatility, *Mathematical Finance: An International Journal of Mathematics, Statistics and Financial Economics* **21**(2): 233–256.